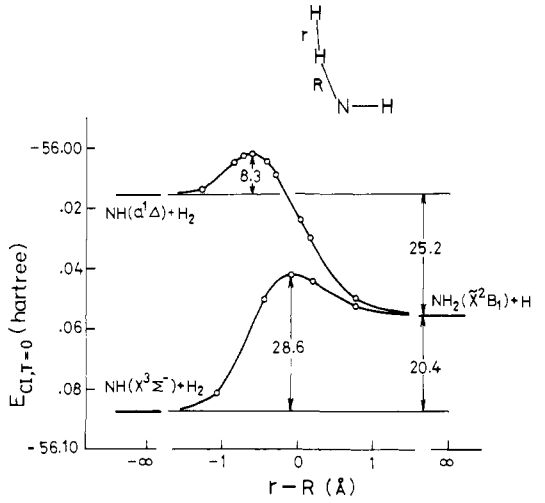

Figure 1. Potential energy profiles calculated for the reactions NH + $H_2 \rightarrow NH_2$ + H. The energy gap values indicated are in units of kcal/mol.

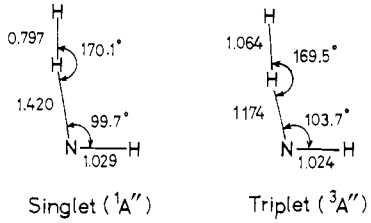

Figure 2. Geometries of the transition states (4-31G CI maxima) for the reactions NH + $H_2 \rightarrow NH_2$ + H. Bond distances are given in units of Å.

reaction path as the transition state (TS). Geometries for the transition states thus located are shown in Figure 2. As for the geometries of NH, H_2, and NH_2, the experimental bond distances and angle have been taken from the literature.[8]

The activation barrier height $\Delta E^{\ddagger}$ calculated for the singlet reaction in question is 8.3 kcal/mol, which is considerably smaller than the value of 28.6 kcal/mol obtained previously for the corresponding triplet reaction.[5] In both cases, the square weight of the open-shell diradical configuration $(1a')^2...(4a')^2(5a')(1a'')$ contributing to the CI-expanded-state function is over 0.93 throughout the course of reaction. The energy change of reaction calculated for the singlet case $\Delta E = -25.2$ kcal/mol agrees reasonably well with the experimental heat of reaction $\Delta H° = -26.1 \pm 3$ kcal/mol.[9,10]

The transition states, both singlet and triplet, as well as the initial and final states of reactions were subjected to the same CI calculations employing the 4-31G** basis functions.[6b] The 4-31G optimized TS geometries were adopted for these calculations. The $\Delta E^{\ddagger}$ and ΔE values obtained were 8.5 and −25.0 kcal/mol, respectively. The effects of the polarization functions have thus proved to be immaterial.

Calculations have been extended to the reaction of methane:

$$NH(a^1\Delta) + CH_4 \rightarrow NH_2(\tilde{X}^2B_1) + CH_3 \qquad (2)$$

Only the 4-31G basis set was used for the sake of computational economy. The lowest configuration-selection threshold used was $T = 10$ μhartree, and the successive four T values increasing stepwise by 10 μhartree each were adopted to obtain the extrapolated CI energy $E_{CI,T\rightarrow 0}$. The transition-state geometry was searched for in exactly the same manner as for the reaction with H_2. The corresponding triplet case has also been dealt with likewise. The transition-state geometries located for both cases are illustrated in Figure 3.

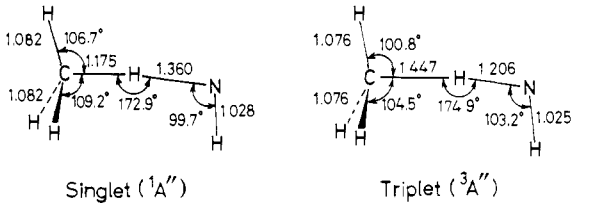

Figure 3. Geometries of the transition states (4-31G CI maxima) for the reactions NH + $CH_4 \rightarrow NH_2 + CH_3$. Bond distances are given in units of Å. The dihedral angles ϕ(HCHN) associated with the out-of-plane hydrogens are 119.5° for both the $^1A''$ and $3A''$ geometries.

The activation barrier height calculated for reaction 2 is $\Delta E^{\ddagger}$ = 13.6 kcal/mol (based on $E_{CI,T\rightarrow 0}$), a value that is noticeably smaller than $\Delta E^{\ddagger}$ = 37.7 kcal/mol obtained for a similar reaction of $NH(X^3\Sigma^-)$. The results are in line with the view[4] that the direct hydrogen abstraction from paraffins by $NH(a^1\Delta)$ in the gas phase is a fairly favorable process in the ordinary temperature region. The relatively large $\Delta E^{\ddagger}$ value obtained for the triplet case negates the possibility that the abstraction is in reality due to $NH(X^3\Sigma^-)$ formed by collisional deactivation of $NH(a^1\Delta)$.

The results of calculation presented herewith seem to serve as an endorsement of the innate capability of $NH(a^1\Delta)$ in entering into direct abstraction of a hydrogen atom from paraffins. Clearly, the radical character of $NH(a^1\Delta)$ is a natural consequence of a dominant contribution of the singlet open-shell-type configuration to its electronic structure. The situation should remain much the same in the case of the $O(^1D)$ atom allowed to react with paraffins.[11]

Acknowledgment. We are grateful to Professor R. J. Buenker for supplying the MRD-CI program. Partial support of this work by the Ministry of Education, Japan (Grant-in-Aid 56340024) is also acknowledged.

Registry No. NH radical, 13774-92-0; H_2, 1333-74-0; CH_4, 74-82-8.

(8) Herzberg, G. "Molecular Spectra and Molecular Structure. III. Electronic Spectra of Polyatomic Molecules"; Van Nostrand: New York, 1966. (b) Huber, K. P.; Herzberg, G. "Molecular Spectra and Molecular Structure. IV. Constants of Diatomic Molecules"; Van Nostrand: New York, 1979.

(9) Calculated on the basis of the experimental heat of formation $\Delta H_f°$ = 3.65 ± 0.10 eV for $NH(X^3\Sigma^-)$: Piper, L. G. *J. Chem. Phys.* **1980**, *72*, 1303.

(10) The heat of reaction was calculated from the relevant data for the heats of formation: Benson, S. W. "Thermochemical Kinetics", 2nd ed.; Wiley: New York, 1976.

(11) Yamazaki, H.; Cvetanović, R. J. *J. Chem. Phys.* **1964**, *41*, 3703.

Selective Enhancement of Tyrosine and Tryptophan Resonance Raman Spectra via Ultraviolet Laser Excitation

Richard P. Rava and Thomas G. Spiro*

Department of Chemistry, Princeton University
Princeton, New Jersey 08544

Received March 14, 1984

The advent of pulsed lasers, capable of generating large photon fluxes in the ultraviolet region, has sparked interest in UV resonance Raman (RR) spectroscopy. In view of the importance of UV chromophores in biology, especially nucleic acid bases, and protein aromatic side chains, the UV RR technique is particularly attractive for biological applications. The technique provides selective enhancement of chromophore vibrational modes and is therefore a discriminating probe of local structure. Ziegler and Hudson have recently reported UV RR spectra of benzene[1] and alkylbenzenes,[2] excited with 212.8-nm radiation obtained by generating the fifth harmonic of the fundamental frequency (1064 nm) of the Nd:YAG laser, which are instructive with respect to the mechanism of vibronic scattering from the forbidden $\pi-\pi^*$

(1) Ziegler, L. D.; Hudson, B. *J. Chem. Phys.* **1981**, *74*, 982.
(2) Ziegler, L. D.; Hudson, B. S. *J. Chem. Phys.* **1983**, *79*, 1134.

0002-7863/84/1506-4062$01.50/0

Table I. Resonance Raman Frequencies of Major Bands of Tyrosine at 200 nm and Tryptophan at 218 nm

tyrosine at 200 nm		tryptophan at 218 nm	
freq	assignment[a,b]	freq	assignment[a,c]
1617	8a	1622	8b
1601	8b	1555	totally symmetry naphthalene-type stretch
1268	7a (C–O stretch)		
1215	para-substituted benzene totally symmetry stretch[d]	1361	sensitive to environement
		1342	pyrrole ring
1184	9a	1241	
858	ring breath		
838	2 × 16a	1016	benzene and pyrrole ring; breath, out of phase
		884	skeletal vibration with appreciable NH pyrrole bend
		762	benzene and pyrrole ring; breath, in phase

[a] Numbering scheme of benzene ring modes comes from: Wilson, E. B., Jr. *Phys. Rev.* **1934**, *45*, 706. [b] Assignments similar to *p*-cresol: Jakobsen, R. J. *Spectrochim. Acta* **1965**, *21*, 433. [c] Assignments from ref 5a. [d] Characteristic band of para-substituted benzenes which has appreciable substituent stretch. See: Dollish, F. R.; Fateley, W. G.; Bentley, F. F. "Characteristic Raman Frequencies of Organic Compounds"; Wiley: New York, 1974.

states. Asher and co-workers[3] have measured benzene excitation profiles in the 220–250-nm region by mixing the Nd:YAG fundamental with the frequency-doubled output of a pulsed dye laser. Person and co-workers[4] have noted preresonance enhancement of tryptophan modes using 363.8-nm irradiation from a cw Ar^+ laser. We now report high-quality RR speectra of the aromatic amino acids tryosine and tryptophan, obtained by using 200- and 218-nm laser excitation, respectively. Light at these wavelengths was generated by focusing the fourth harmonic (266 nm) line from a Nd:YAG laser into a 1-m cell filled with H_2 (7 atm), which shifts the laser frequency via stimulated Raman processes. The spectra show good signal to nosie at low concentrations (10^{-3} M) and surprisingly high selectivity for the two chromophores.

Figure 1 shows RR spectra of tyrosine (a) and tryptophan (d), using 200- and 218-nm irradiation, respectively, and compares them with spectra of tryptophyltyrosine at these two wavelengths (b and c). All solutions were $\sim 10^{-3}$ M, 2–3 orders of magnitude more dilute than the concentrations typically required for nonresonance Raman spectroscopy. The RR bands correspond to several ring modes of each of the chromophores, which have been assigned in nonresonance Raman spectra[5] (see Table I). At 200 nm the dipeptide spectrum shows tyrosine modes exclusively. There are only hints of the most intense of tryptophan modes at 763, 1016, and 1555 cm^{-1}. At 218 nm, the spectrum is dominated by tryptophan, although weak tyrosine scattering can be seen at 1184 and 1620 cm^{-1}.

Like benzene, tyrosine and tryptophan have two (largely) forbidden $\pi-\pi^*$ electronic transitions below the first-allowed transition.[6] The forbidden transitions are capable only of relatively weak enhancement of modes which are effective in mixing the forbidden and allowed transitions, as demonstrated for benzene and alkylbenzenes by Ziegler and Hudson.[1,2] Allowed transitions, however, produce strong enhancements of symmetric modes with large displacements in the excited state. The 218-nm laser line falls in the second forbidden transition of tyrosine (λ_{max} = 222 nm), but it is within the allowed absorption band of tryptophan (λ_{max} = 218 nm, ϵ = 34 000 M^{-1} cm^{-1}). It is therefore not surprising that the RR spectrum is dominated by ring modes of tryptophan. The 200-nm line is within the allowed absorption

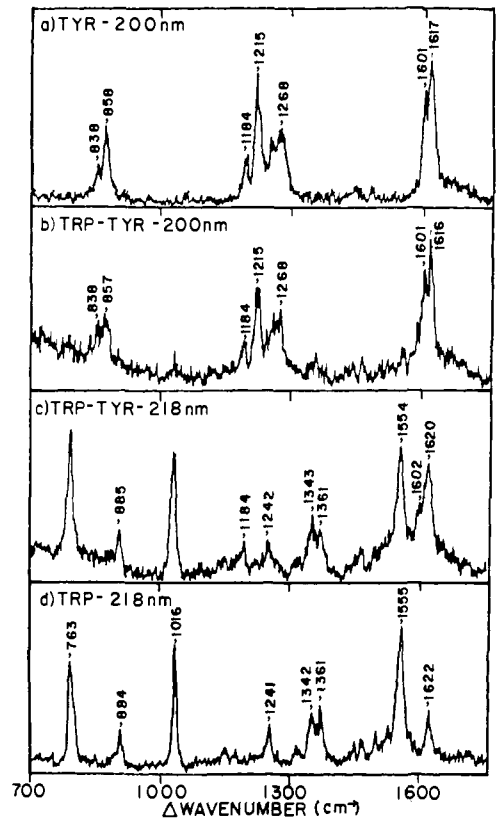

Figure 1. Raman spectra in the ring-mode region for aqueous solutions of (a) tyrosine (10^{-3} M), (b) and (c) tryptophyltyrosine (10^{-3} M), and (d) tryptophan (10^{-3} M). Excitation at the indicated wavelengths is provided by pulsed-laser excitation obtained via H_2-Raman shifting the 266-nm fourth harmonic output of a Q-switched Nd:YAG laser to the second (218 nm) and third (200 nm) anti-Stokes levels. The laser pulses were focused onto a free-flowing stream of the sample solution,[1] and the Raman photons were analyzed with a monochromator equipped with a solar blind phototube. The accuracy of the band frequencies is estimated to be ±2 cm^{-1}.

band of tyrosine (λ_{max} = 193 nm, ϵ = 36 000 M^{-1} cm^{-1}), and several tyrosine ring modes are now enhanced. What is surprising, however, is the disappearance of the tryptophan modes at 200 nm, since the absorptivity of tryptophan remains high (ϵ = 20 900 M^{-1} cm^{-1}) at this wavelength. We tentatively ascribe this phenomenon to interference effects in the Raman polarizability tensor associated with higher lying excited states.[7]

The high degree of discrimination between tyrosine and tryptophan augurs well for UV RR studies of proteins. It should be possible, by using 200 and 218 nm excitation, to study either tyrosine or tryptophan in the same protein, without interference from the other. The RR spectra contain bands that are known to be sensitive to the environment of the chromophore. The tyrosine doublet at $\sim$850 cm^{-1}, which results from a Fermi resonance between the tyrosine ring breathing mode and the overtone of an out-of-plane deformation, is known to show large variations in the relative intensities of the two components, dependent on H-bonding effects.[8] This doublet is clearly revealed in the 200-nm spectra of tyrosine and tryptophyltyrosine. Nonresonance Raman studies have shown that a tryptophan band at 1360 cm^{-1} sharpens in hydrophobic environments.[9] The 218-nm spectra reveal a doublet at 1360 cm^{-1}; in the nonresonance Raman spectra this doublet structure is difficult to quantitate.[5b] In addition, the 884-cm^{-1} mode, which has a large contribution of pyrrole NH bending, has been observed in protein nonresonance

(3) Asher, S. A.; Johnson, C. R.; Murtaugh, J. *Rev. Sci. Instrum.* **1983**, *54*, 1657.
(4) Brown, K. G.; Brown, E. B.; Person, W. B. *J. Am. Chem. Soc.* **1977**, *99*, 3128.
(5) (a) Hirakawa, A. Y.; Nishimura, Y.; Matsumoto, T.; Nakanishi, M.; Tsuboi, M. *J. Raman Spectrosc.* **1978**, *7*, 282. (b) Lord, R. C.; Yu, N.-T. *J. Mol. Biol.* **1970**, *50*, 509.
(6) Hooker, T. M., Jr.; Schellman, J. A. *Biopolymers* **1970**, *9*, 1319.
(7) See, for example: Stein, P.; Miskowski, V.; Woodruff, W. H.; Griffin, J. P.; Werner, K. G.; Gaber, G. P.; Spiro, T. G. *J. Chem. Phys.* **1976**, *64*, 2159.
(8) Siamwiza, M. N.; Lord, R. C.; Chen, M. C.; Takamatsu, T.; Harada, I.; Matsuura, H.; Shimanouchi, T. *Biochemistry* **1975**, *14*, 4870.
(9) Chen, M. C.; Lord, R. C., Mendelsohn, R. *Biochim. Biophys. Acta* **1973**, *328*, 252.

Raman to become stronger when tryptophan is in a hydrophobic region.[10]

It seems quite likely that the highly resolved RR spectra of these chromophores will reveal additional spectroscopic signatures of the local environment of the chromophores. We have observed, for example, that the tyrosine doublet at 1610 cm^{-1} shifts to lower frequency upon deprotonation.

Acknowledgment. This work was supported by NSF Grant CHE-8106984 and NIH Grant GM25158. R.P.R. is the recipient of a postdoctoral research fellowship NIH 5 F32 GM 09104-02.

(10) Kitagawa, T.; Azuma, T.; Hamaguchi, K. *Biopolymers* **1979**, *18*, 451.

π-Accepting Abilities of Phosphines in Transition-Metal Complexes

Dennis S. Marynick

Department of Chemistry
The University of Texas at Arlington
Arlington, Texas 76019-0065
Received January 25, 1984

A recent paper[1] described in some detail the nature of the frontier orbitals in PX_3 systems, with X = H, CH_3, or F. The authors concluded that "the π-acceptor orbital on phosphorus mostly consists of phosphorus 3p character".[2] Their conclusions were based on Xα calculations on the free ligands. Here, we use approximate[3] and ab initio molecular orbital theory to demonstrate π accepting in phosphine ligands *without involving d orbitals on phosphorus* in actual transition-metal complexes.

Our own interest in this subject arose from a study of cis–trans isomerization energies in systems such as $Cr(NH_3)_4(CO)_2$ and $Cr(PH_3)_4(CO)_2$.[4] Simple π-bonding arguments lead one to predict that $Cr(NH_3)_4(CO)_2$ should exist in the cis conformation, since only that conformation allows π back-bonding to the carbonyls from all three occupied t_{2g} orbitals[5] (assuming NH_3 cannot act as a π acceptor).[6] Indeed, the cis complex is calculated by the PRDDO method[3] to be 13.4 kcal/mol more stable than the trans isomer,[7] and its enhanced stability can be traced directly to greater π back-bonding.[8] A similar PRDDO calculation on *cis*- and *trans*-$Cr(PH_3)_4(CO)_2$ without d orbitals on phosphorus predicts the cis isomer to be only 0.3 kcal/mol more stable than the trans arrangement.[9] Analysis of the wave functions shows that the enhanced stability of *trans*-$Cr(PH_3)_4(CO)_2$ relative to the cis isomer is due to the fact that *the phosphine ligands are acting as π acceptors even though no d orbitals are included in the phosphorus basis set.* Thus, all three t_{2g} orbitals are stabilized by π back-bonding in both conformations of the phosphine complex,[10] reducing the energy difference between the two isomers.

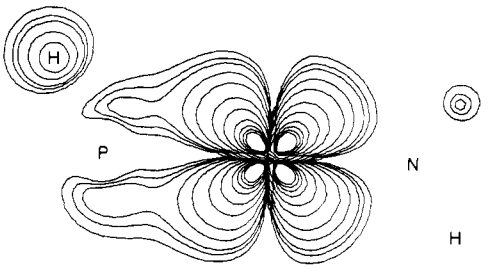

Figure 1. Electron density plot of one of the two π-donating d orbitals in $Cr(NH_3)_5(PH_3)$ without d orbitals on phosphorus. The contour levels are 0.5, 0.4, 0.3, 0.2, 0.1, 0.05, 0.02, 0.01, 0.005, 0.0035, and 0.002 e/au^3.

To further quantify the π-accepting ability of phosphine without d orbitals a PRDDO calculation on the model complex $Cr(NH_3)_5(PH_3)$ was performed, with the phosphine on the *z* axis. No d orbitals were included in the phosphorus basis set. The resultant d-orbital populations on Cr were 1.80 e (d_{xz} and d_{yz}) and 1.97 e (d_{xy}). Examination of the phase relationships among the hydrogen, phosphorus, and chromium orbitals shows that the π-accepting orbital on phosphine has local σ^* symmetry with respect to the P–H bond axis.[11] An electron density plot of one of the two d_π orbitals is presented in Figure 1. Additional evidence for σ^* participation comes from the P–H overlap populations. Substantial population of the P–H σ^* orbital in the complex should lower the P–H overlap population relative to free phosphine. Indeed, the P–H overlap populations of the free and complexed ligand are 0.61 and 0.51, respectively.

To test the relative importance of σ^* vs. 3d orbitals in π accepting, we have performed ab initio calculations on the model tetrahedral complex $Ni(NH_3)_3(PH_3)$ with a double-ζ basis set with and without d orbitals on the phosphorus.[12] PRDDO-optimized geometries were employed.[13] This complex is formally d^{10}, and if the phosphine is placed on the *z* axis, the d_{xz} and d_{yz} orbitals should be depopulated relative to d_{xy} and $d_{x^2-y^2}$.[14] Indeed, without d orbitals on phosphorus, the relevant d-orbital populations on Ni are d_{xz}, d_{yz} (1.60 e) and d_{xy}, $d_{x^2-y^2}$ (1.74 e). Significant delocalization is seen from the metal d's to the phosphine hydrogens (0.30 e) and the phosphorus (0.13 e), but not to the amine hydrogens or nitrogen (0.01 e).[15] Addition of a d orbital to the phosphorus changes the Ni d-orbital populations only very slightly: d_{xz}, d_{yz} (1.57 e), and d_{xy}, $d_{x^2-y^2}$ (1.76 e); however, the group charge on PH_3 (defined as the sum of the orbital populations of all orbitals on phosphine) is exactly the same in the polarized and unpolarized calculations.

It is well-known that PF_3 is a better π acceptor than PH_3. The textbook explanation[16] is that electronegative substituents lower the energy of the d orbitals on phosphorus and therefore make them more available for bonding; however, π accepting into σ^*

(1) Xiao, S.; Trogler, W. C.; Ellis, D. E.; Berkovitch-Yellin, Z. *J. Am. Chem. Soc.* **1983**, *105*, 7033.

(2) This conclusion was explicity stated for PF_3, but also holds for PH_3.

(3) Halgren, T. A.; Lipscomb, W. N. *J. Chem. Phys.* **1973**, *58*, 1569. Marynick, D. S.; Lipscomb, W. N. *Proc. Natl. Acad. Sci. U.S.A.* **1982**, *79*, 1341.

(4) Marynick, D. S.; Askari, S.; Nickerson, D. F., manuscript in preparation.

(5) For convenience, we employ octahedral symmetry notation.

(6) Only two d orbitals are π bonding in the trans isomer.

(7) The basis sets for these calculations are given in: Marynick, D. S.; Kirkpatrick, C. M. *J. Phys. Chem.* **1983**, *87*, 3273. The geometries were optimized.

(8) For the cis isomer, with carbonyls on the *z* and *y* axes, the d-orbital populations are d_{xz} (1.80), d_{yz} (1.19), and d_{xy} (1.80). For the trans isomer, with carbonyls on the *z* axis, the corresponding populations are 1.45, 1.45, and 1.99.

(9) The phosphine complex is known to exist in the cis form: Hutter, G.; Schelle, S. J. *Cryst. Mol. Struct.* **1971**, *1*, 69.

(10) The d-orbital populations for the *cis*-phosphine complex are d_{xz} (1.69), d_{yz} (1.35), and d_{xy} (1.69). For the trans complex the corresponding values are 1.44, 1.44, and 1.87. The significant reduction of the d_{xy} population of the *trans*-phosphine complex relative to that of the *trans*-amine complex is a direct manifestation of the π-accepting ability of PH_3, even without d orbitals.

(11) In ref 1, the π-accepting orbitals are described as simply being dominately 3p, but the wave function plots clearly identify the orbitals as having local σ^* symmetry. Participation of σ^* orbitals in some organophosphorus systems has been discussed previously: Gray, G. A.; Albright, T. A. *J. Am. Chem. Soc.* **1977**, *99*, 3243. Earlier qualitative discussions of bonding in similar systems appear in: Hoffmann, R.; Boyd, D.; Goldberg, S. Z. *J. Am. Chem. Soc.* **1970**, *92*, 3929. The π-accepting utility of the lowest unoccupied orbital of e symmetry in calculations without d orbitals on phosphorus has been briefly noted by: Yarbrough, L. W.; Hall, M. B. *Inorg. Chem.* **1978**, *17*, 2269.

(12) The basis set, which is minimal for the inner shells and double-ζ for the valence shells (including the metal 3d), will be fully described in ref 4. We have repeated these calculations with two d orbitals on phosphorus and find no significant differences.

(13) *R*(Ni–N) = 2.012 Å and *R*(Ni–P) = 1.981 Å, tetrahedral angles assumed. Note that the exceptionally short Ni–P distance is another manifestation of π back-bonding. The ab initio calculations were repeated with the Ni–P bond lengthened by 0.13 Å, with no significant differences.

(14) With respect to the phosphine, the d_{xz} and d_{yz} orbitals are π bonding, while the d_{xy} and $d_{x^2-y^2}$ orbitals have local δ symmetry.

(15) The orbital populations quoted here represent the electron delocalization from the four MO's which are dominately d_{xy}, $d_{x^2-y^2}$, d_{xz}, and d_{yz}. The phase relationships among the phosphine orbitals are clearly consistent with σ^* π acceptance.

(16) See, for instance: Huheey, J. E. "Inorganic Chemistry"; Harper and Row: New York, 1983; pp 832–833.

0002-7863/84/1506-4064$01.50/0